JOURNAL OF SOLID STATE CHEMISTRY **92**, 219–226 (1991)

Completion of the Alkali Metal Titanium (III) Pyrophosphate Series: Synthesis and Structure of $A^{I}TiP_2O_7$ (A^{I} = K, Rb, Cs)

SHUMIN WANG AND SHIOU-JYH HWU*

Department of Chemistry, Rice University, P.O. Box 1892, Houston, Texas 77251

Received August 13, 1990; in revised form December 26, 1990

The structure of a new titanium (III) pyrophosphate $RbTiP_2O_7$ has been determined. It crystallizes in a monoclinic unit cell ($P2_1/c$, $Z = 4$) with dimensions $a = 7.542$ (7) Å, $b = 10.256$ (2) Å, $c = 8.270$ (3) Å, $\beta = 105.59$ (5)°, $V = 616.2$ (6) Å^3. The single crystal structure refinement gives a final structure solution with R index on F_0^2 of 0.046 for 101 variables and GOF = 1.76. $RbTiP_2O_7$ is isostructural with $KAlP_2O_7$, whose structure is also adopted by trivalent transition metal containing pyrophosphates; namely $M^{I}MoP_2O_7$ (M^{I} = K, Rb, and Cs) and $KFeP_2O_7$. The potassium and cesium analogues are also synthesized. The structure differences between $LiTiP_2O_7$, $NaTiP_2O_7$ (β-phase), and (K,Rb,Cs)TiP_2O_7 are contrasted by the connectivity of the TiO_6 octahedra and P_2O_7 pyrophosphate groups. The structural relationship between $RbTiP_2O_7$ and previously reported $BaTi_2(P_2O_7)_2$ versus the role of electropositive cations in the formation of $Ti(P_2O_7)_nO_{6-2n}$ units (n is 1 for Rb^+ and 2 for Ba^{2+}) are discussed.

Introduction

Pseudoternary titanium phosphates form a number of structurally interesting compounds that consist of mixed frameworks of AO_m polyhedra (A = mono- or divalent electropositive cations, $m = 4 \sim 10$), TiO_6 octahedra, and PO_4 tetrahedra. The combination of complex interactions of metal-oxide polyhedra and the multivalency of titanium cations has resulted in many new compounds that possess framework structures with sizable tunnels. Recently we have reported a new compound $BaTi_2(P_2O_7)_2$ (*1*), whose framework is characterized by tunnel structures which contain barium cations. In the structural unit of $[Ti(P_2O_7)_2O_2]$, the two "bidentate" pyrophosphate P_2O_7 ligands share corner oxygen atoms with the TiO_6 octahedron in a *cis* configuration. In the publication, we also noted that the use of rigid and bulky oxyanions resulted in compounds characterized by structurally isolated and electronically localized $Ti^{3+}(d^1)$ cations. This type of compound offers a great opportunity for an examination of the physical properties associated with reduced titanium cations, because the interaction between the neighboring cations is simplified.

In searching for new compounds to understand the role of the electropositive cations in the structural framework formation, we have studied the system $A^{I}TiP_2O_7$. In this series, only α- and β-sodium titanium (III) pyrophosphates are known (*2*). Our investigations show that different size alkali metal cations also allow $A^{I}TiP_2O_7$-type compounds to form with different structural

* To whom correspondence should be addressed.

0022-4596/91 $3.00

frameworks. We also found that the structures of the Li (*3*), β-Na and (K,Rb,Cs) TiP_2O_7 compounds are related to that of the iron (III) pyrophosphate series (*4*). In this paper we describe the structure of rubidium titanium (III) pyrophosphate, $RbTiP_2O_7$, and the differences in structure connectivity compared with the pyrophosphates containing smaller alkali metal cations. The synthesis of the potassium and cesium analogues and the structure comparison with $BaTi_2(P_2O_7)_2$ are also discussed.

Experimental

Synthesis. Purplish-blue gem crystals of $RbTiP_2O_7$ were discovered in the reaction products formed in an attempt to synthesize "$RbTiP_3SiO_{11}$." The reaction mixture of Aldrich Rb_2CO_3 (99.9%), TiO_2 (99.9+%), and SiO_2 (99.995+%) and $(NH_4)_2HPO_4$ (Fisher Scientific Co., 99.4%) were mixed in a mole ratio of 1 : 1 : 2 : 6 followed by calcination in air at 800°C to prepare a precursor with the nominal composition of "$Rb_2TiP_6Si_2O_{22}$." This mixture was then added to an equimolar titanium metal powder (Aldrich, 99.9%) in an evacuated silica tube. The reaction was heated at 1000°C for 72 hr followed by slow cooling at a rate of −5°C/hr to 550°C then −10°C/hr to room temperature. After the structure determination, the synthesis of pure phase $RbTiP_2O_7$ was performed, stoichiometrically, using the previously described procedure (*1*). The nominal composition of the precursor was "$RbTi_{3/4}P_2O_7$." The calcination temperature was 800°C. The stoichiometric reaction took place at 1000°C followed by furnace cooling to room temperature. A large yield of polycrystalline $RbTiP_2O_7$ was obtained.

TABLE I

CRYSTAL DATA FOR $RbTiP_2O_7$

Formula mass (amu)	307.31
Space group	$P2_1/c$ (No. 14)
a (Å)	7.542 (7)
b (Å)	10.256 (2)
c (Å)	8.270 (3)
β (degree)[a]	105.59 (5)
V (Å^3)	616.2 (6)
Z	4
T (K) of data collection	296
D calculated (g cm^{-3})	3.92
Radiation (graphite monochromated)	Mo$K\alpha$ (λ = 0.71069 Å)
Crystal shape, color	Gem-like, purplish-blue
Crystal size (mm)	0.15 × 0.20 × 0.20
Linear abs. coeff. (cm^{-1})	99.053
Transmission factors	0.74–1.00
Scan type	ω–2θ
Scan speed (deg/min)	4.0
Scan range (deg)	−0.7 to 0.7° in ω
Background counts	¼ of scan range on each side of reflection
2θ (max) (deg)	55
Data collected	$+h, \pm k, \pm l$
p for $\sigma(F^2)$	0.03
No. of unique data ($F_0^2 > 0$)	944
No. of unique data with $F_0^2 > 3\sigma(F_0^2)$	859
F_{000}	580
$R(F^2)$	0.046
$R_w\ (F^2)$	0.060
R (on F for $F_0^2 > 3\sigma(F_0^2)$)	0.088
2nd extinction coefficient (10^{-7})	2.36
No. of variables	101
Error in observation of unit weight (e^2)	1.76

[a] α and γ were constrained to be 90° in the refinement of cell constants.

Single crystal X-ray structure determination. A gem crystal, with average dimensions 0.15 × 0.20 × 0.20 mm, was selected for indexing and intensity data collection on a Rigaku AFC5S four circle diffractometer (Mo$K\alpha$ radiation, λ = 0.71069 Å) equipped with a graphite monochrometer. Crystallographic data collection parameters are tabulated in Table I. Empirical absorption corrections were based on three (2θ = 18.09°,

TABLE II

Positional and Equivalent Thermal Parameters for $RbTiP_2O_7$

Atom	Wyckoff notation	Atomic parameters x	y	z	$B_{(eq)}(Å^2)^a$
Rb	4e	0.1889(2)	0.6855(1)	0.5519(2)	1.51(5)
Ti	4e	0.2367(3)	0.3996(2)	0.2591(3)	0.53(8)
P(1)	4e	0.4366(4)	0.1348(3)	0.1869(4)	0.5(1)
P(2)	4e	0.1324(4)	0.0970(3)	0.3292(4)	0.6(1)
O(1)	4e	0.446(1)	0.2792(8)	0.232(1)	0.9(3)
O(2)	4e	0.322(1)	0.1059(9)	0.010(1)	1.2(3)
O(3)	4e	0.629(1)	0.0765(8)	0.227(1)	0.7(3)
O(4)	4e	0.330(1)	0.0610(8)	0.305(1)	0.7(3)
O(5)	4e	0.082(1)	0.2330(8)	0.261(1)	0.9(3)
O(6)	4e	0.000(1)	−0.0026(8)	0.228(1)	0.8(3)
O(7)	4e	0.150(1)	0.0864(9)	0.513(1)	1.1(3)

Atom	Thermal parameters[b] U_{11}	U_{22}	U_{33}	U_{12}	U_{13}	U_{23}
Rb	0.0163(7)	0.0227(7)	0.0165(7)	0.0004(6)	0.0017(5)	−0.0036(6)
Ti	0.007(1)	0.007(1)	0.005(1)	0.0002(9)	0.0011(8)	−0.0004(8)
P(1)	0.005(1)	0.005(1)	0.009(1)	0.001(1)	0.003(1)	0.000(1)
P(2)	0.007(2)	0.008(2)	0.008(1)	−0.003(1)	0.003(1)	−0.000(1)
O(1)	0.011(4)	0.007(4)	0.018(5)	−0.001(3)	0.006(4)	−0.002(4)
O(2)	0.011(4)	0.019(5)	0.013(4)	0.000(4)	0.002(4)	0.004(4)
O(3)	0.009(4)	0.004(4)	0.014(4)	0.004(3)	0.005(3)	0.002(3)
O(4)	0.006(4)	0.015(5)	0.009(4)	−0.003(3)	0.006(3)	0.002(3)
O(5)	0.015(4)	0.012(4)	0.009(4)	−0.001(4)	0.006(3)	0.001(4)
O(6)	0.014(4)	0.009(4)	0.007(4)	−0.000(4)	0.004(3)	0.000(3)
O(7)	0.013(5)	0.018(5)	0.007(4)	−0.006(4)	−0.004(3)	−0.003(4)

[a] Anisotropically refined atoms are given in the form of the isotropic equivalent displacement parameter defined as $B_{eq} = \frac{4}{3}[a^2\beta_{11} + b^2\beta_{22} + c^2\beta_{33} + (2ac\cos\beta)\beta_{13}]$.

[b] The general temperature-factor expression of an atom for a given set of planes (hkl) is $\exp[-2\pi^2(U_{11}h^2a^{*2} + U_{22}k^2b^{*2} + U_{33}l^2c^{*2} + 2U_{13}hla^*c^*\cos\beta^*)]$, where the U_{ij} are the thermal parameters expressed in terms of mean-square amplitudes of vibration in angstroms.

22.43°, and 29.43°) azimuthal scans. The Laue patterns showed monoclinic symmetry ($2/m$). There was no detectable decay according to three standard reflections (2 0 0, 1 0 −2, 2 −1 −2) that were measured every 100 reflections during data collection. Data reduction, intensity analysis, space group determination and single crystal structure refinement were accomplished with the procedure previously described (*1*). The atomic coordinates were found using the program SHELX-86 (*5*), and later proven to be similar to that of $KAlP_2O_7$ (*6*). The occupancy factor for rubidium atoms was initially refined but the resultant value, 0.98 (1), indicated full occupancy. Inclusion of a secondary extinction correction, owing to the gem shape geometry, did not seem to affect the result of the structure refinement. The final positional and thermal parameters

TABLE III

IMPORTANT BOND DISTANCES (Å) AND ANGLES (deg) FOR $RbTiP_2O_7$

	TiO_6 octahedron		
Ti–O(1)	2.067(8)	Ti–O(5)	2.070(8)
Ti–O(2)	1.998(8)	Ti–O(6)	2.076(8)
Ti–O(3)	2.066(8)	Ti–O(7)	1.970(8)
O(1)–Ti–O(6)	171.4(3)	O(2)–Ti–O(3)	87.1(3)
O(2)–Ti–O(7)	177.4(4)	O(2)–Ti–O(5)	89.7(3)
O(3)–Ti–O(5)	173.1(3)	O(2)–Ti–O(6)	90.2(3)
O(1)–Ti–O(2)	93.1(4)	O(3)–Ti–O(6)	89.3(3)
O(1)–Ti–O(3)	98.8(3)	O(3)–Ti–O(7)	90.9(3)
O(1)–Ti–O(5)	87.5(3)	O(5)–Ti–O(6)	84.6(3)
O(1)–Ti–O(7)	88.9(3)	O(5)–Ti–O(7)	92.1(4)
		O(6)–Ti–O(7)	88.1(3)
	PO_4 tetrahedra in P_2O_7 units		
P(1)–O(1)	1.524(8)	P(2)–O(4)	1.599(8)
P(1)–O(2)	1.517(8)	P(2)–O(5)	1.514(9)
P(1)–O(3)	1.521(8)	P(2)–O(6)	1.514(8)
P(1)–O(4)	1.611(8)	P(2)–O(7)	1.493(8)
O(1)–P(1)–O(2)	113.75(5)	O(4)–P(2)–O(5)	108.3(5)
O(1)–P(1)–O(3)	110.3(5)	O(4)–P(2)–O(6)	105.8(5)
O(1)–P(1)–O(4)	108.0(5)	O(4)–P(2)–O(7)	106.3(5)
O(2)–P(1)–O(3)	113.2(5)	O(5)–P(2)–O(6)	110.7(5)
O(2)–P(1)–O(4)	104.4(5)	O(5)–P(2)–O(7)	113.0(5)
O(3)–P(1)–O(4)	106.6(5)	O(6)–P(2)–O(7)	112.3(5)
	P(1)–O(4)–P(2)	127.0(5)	
	RbO_{10} polyhedron		
Rb^a $-O(1)^c$	2.874(9)	Rb^a $-O(5)^a$	2.878(9)
$-O(2)^d$	3.203(9)	$-O(5)^c$	2.997(9)
$-O(3)^b$	3.186(8)	$-O(6)^d$	2.963(8)
$-O(3)^c$	3.137(8)	$-O(6)^e$	3.055(8)
$-O(4)^d$	3.273(8)	$-O(7)f$	3.399(9)
$O(1)^c-O(3)^c$	2.50(1)	$O(3)^c-O(5)^c$	3.72(1)
$O(1)^c-O(4)^d$	3.40(1)	$O(4)^d-O(6)^d$	2.48(1)
$O(2)^d-O(4)^d$	2.47(1)	$O(5)^a-O(6)^e$	2.49(1)
$O(2)^d-O(3)^b$	2.80(1)	$O(5)^a-O(7)f$	2.91(1)
$O(2)^d-O(6)^e$	2.89(1)	$O(5)^c-O(7)^f$	2.51(5)
$O(2)^d-O(6)^d$	3.57(1)	$O(5)^c-O(6)^d$	2.79(1)
$O(3)^b-O(6)^e$	2.91(1)	$O(6)^d-O(6)^e$	3.77(2)
$O(3)^b-O(5)^a$	3.72(1)		

[a] x, y, z.
[b] $1 - x, \frac{1}{2} + y, \frac{1}{2} - z$.
[c] $1 - x, 1 - y, 1 - z$.
[d] $x, \frac{1}{2} - y, \frac{1}{2} + z$.
[e] $-x, \frac{1}{2} + y, \frac{1}{2} - z$.
[f] $-x, 1 - y, 1 - z$.

TABLE IV
LATTICE PARAMETERS OF $A^{I}TiP_2O_7$ (A^I = K, Rb, Cs)

	$KTiP_2O_7$	$RbTiP_2O_7$	$CsTiP_2O_7$
a (Å)	7.400(2)	7.535(3)	7.745(1)
b (Å)	10.258(3)	10.244(3)	10.216(2)
c (Å)	8.208(2)	8.256(3)	8.369(1)
β (degree)[a]	106.26(4)	105.76(6)	104.73(1)
V (Å^3)	598.2(3)	613.3(4)	640.4(2)

[a] α and γ were constrained to be 90° in the refinement of cell constants.

are listed in Table II[1] and the selected bond distances are listed in Table III.

Isotypic compounds. Although $RbTiP_2O_7$ is used for the majority of structure description and discussion, the syntheses of the potassium and cesium analogues were also successful. Pure phases could be prepared by using similar experimental conditions. Polycrystalline samples were identified from their powder X-ray diffraction patterns (XRD; Cu$K\alpha$ radiation, λ = 1.5418 Å). The lattice parameters were obtained by a least squares refinement of twenty reflections (10° $\leq 2\theta \leq$ 60°) with the program LATT (*7*). The refined parameters are listed in Table IV. The cell volumes of the three isotypic compounds are in good agreement with the size of the univalent cations.

Description of Structure and Discussion

$RbTiP_2O_7$ is isostructural with $KAlP_2O_7$ (*6*), whose structure is also adopted by A^I MoP_2O_7 (A^I = K [8*a*], Rb [8*b*], and Cs [8*c*]) and $KFeP_2O_7$ [4*c*]. The framework possesses corner sharing TiO_6 octahedra and pyrophosphate P_2O_7 groups. The unit cell consists of four rubidium atoms, each of which is surrounded by an irregular polyhedron of 10 oxygen atoms. The extended structure projected along the c axis is shown in Fig. 1. The TiO_6 octahedra (in which titanium atoms are in solid circles) form an array that is approximately parallel to the (220) plane. These TiO_6 octahedra are inter-

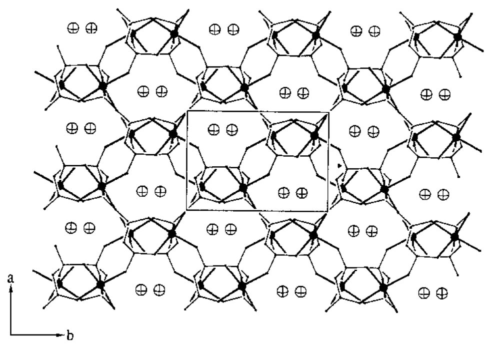

FIG. 1. The ball (titanium atoms) and stick drawing of the extended structure shows the connectivity of the rubidium titanium (III) pyrophosphate framework. The rubidium cations (drawn in large crossed circles) are in the tunnel perpendicular to the ab plane. The Ti–O bonds are represented by the thick lines. The projected unit cell on the ab plane is outlined.

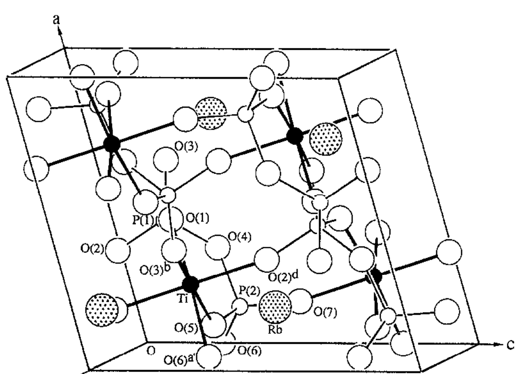

FIG. 2. The unit cell structure of $RbTiP_2O_7$. a': x, $1 + y$, z.

[1] See NAPS Document No. 04842 for 7 pages of supplementary materials from ASIS/NAPS, Microfiche Publications, P.O. Box 3513, Grand Central Station, New York, NY 10163. Remit in advance $4.00 for microfiche copy or for photocopy, $7.75 up to 20 pages plus $.30 for each additional page. All orders must be prepaid.

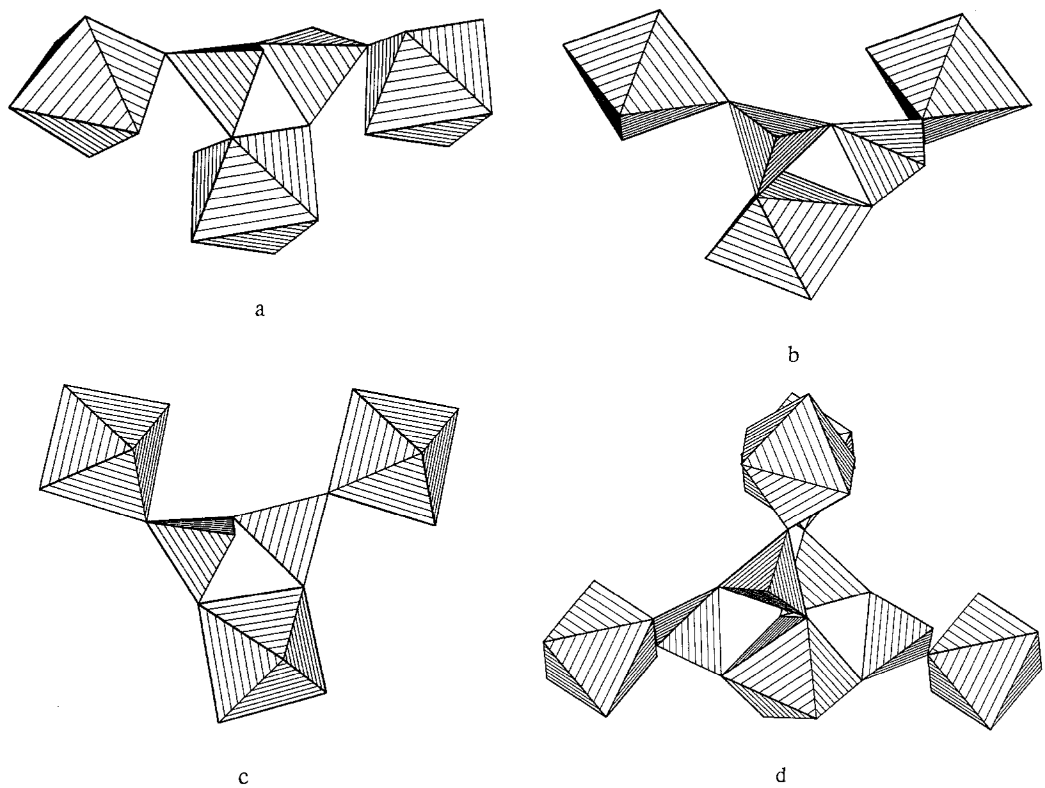

FIG. 3. The *STRUPLO-86* representation of the connectivities of the TiO_6 octahedra and P_2O_7 pyrophosphate groups (viewed along the *c* axis) in (a) $LiTiP_2O_7$, (b) β-$NaTiP_2O_7$, and (c) $RbTiP_2O_7$. For clarity, only two of the four P_2O_7 units connected to TiO_6 octahedra are shown. (d) For comparison, the connection in $BaTi_2(P_2O_7)_2$ is also shown (see text).

connected by the pyrophosphate P_2O_7 groups forming a three-dimensional (3-D) structure. The resulting titanium pyrophosphate framework is characterized by tunnel structures which are perpendicular to the *ab* plane and contain electropositive rubidium cations.

The unit cell structure of $RbTiP_2O_7$ is shown in Fig. 2, with Ti–O bonds drawn in thick lines and P–O bonds in thin lines. The 3-D framework structure can be viewed as each TiO_6 octahedron sharing two of its waist oxygen atoms, O(1) and O(5), with P_2O_7 forming the $[Ti(P_2O_7)O_4]$ unit. In addition, four symmetry-related units in each unit cell are fused through the sharing of the remaining terminal oxygen atoms of P_2O_7, e.g., O(2), O(3), O(6), O(7), to yield a 3-D framework. The averaged Ti–O and P–O bond distances of the title phase, listed in Table III, are comparable to those observed in all three different types of reduced titanium (III) pyrophosphates.

The size effect of the alkali metal cations (A^I) gives rise to the variation in framework structures of the $A^ITiP_2O_7$ series. The size of the monovalent cations determines the geometry of the tunnels which are formed by the AO_m polyhedron ($m = 4$ for Li, 8 for Na, and 10 for K, Rb, and Cs) of the titanium

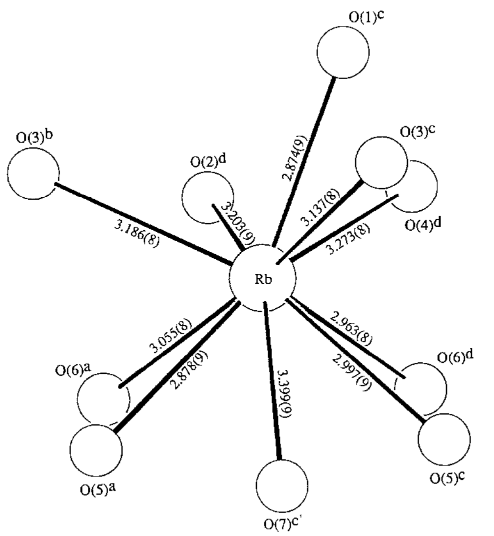

FIG. 4. The coordination of oxygen atoms around Rb^{1+} in $RbTiO_2O_7$. c': $-x$, $1 - x$, $-z$.

pyrophosphate frameworks. In Figs. 3a–3c we show the partial structures of three structure types, namely $LiTiP_2O_7$, β-$NaTiP_2O_7$, and $RbTiP_2O_7$, in order to demonstrate how the size effect profoundly influences the structure arrangement. Each structure possesses a $[Ti(P_2O_7)O_4]$ unit in which one pyrophosphate shares two oxygen atoms (one from each PO_4 tetrahedron) with a TiO_6 octahedron. Two in-plane TiO_6 octahedra connected to the bidentate P_2O_7 group are shown, while the other two (one up and one down) are not shown for clarity. This arrangement is in contrast to what is found in $BaTi_2(P_2O_7)_2$, where the structure unit $[Ti(P_2O_7)_2O_2]$ contains two P_2O_7 groups sharing oxygen atoms with the two *cis* edges of a TiO_6 octahedron (Fig. 3d). Connected to the $Ti(P_2O_7)_2O_2$ unit structure are four of the six non-symmetry-related TiO_6 octahedra [each of which shares corner oxygen atoms with six P_2O_7 groups (*1*)]. Two terminal oxygens, closer to the unit structure, are connected to two symmetry-related $Ti(P_2O_7)_2O_2$ units. The difference in structure connectivity, i.e., $Ti(P_2O_7)_nO_{6-2n}$ (n is 1 for Rb+ and 2 for Ba^{2+}), is attributed in part to the charge effect (e.g., monovalent vs divalent electropositive cations).

The rubidium cations are coordinated to 10 oxygens, at distances ranging from 2.874 to 3.399 Å. This wide distribution in bond length is attributed to the complex electrostatic interaction and to the steric effect of the P_2O_7 group. Four edges of the pyrophosphate group are shared with that of the RbO_{10} polyhedron. The shared edges (2.47 ~ 2.51 Å) are significantly shorter than the unshared edges, e.g., the shortest unshared edge is 2.79 (1) Å. This leads to a considerable distortion of the RbO_{10} polyhedron, as shown in Fig. 4. In terms of electrostatic interaction, induced by different cations with respect to oxygen atoms, all the oxygen atoms in this structure are coordinated to three cations. They are Rb, Ti, and P for terminal oxygens and Rb, P (1), and P (2) for bridging oxygens in the P_2O_7 ligand.

In conclusion, we have demonstrated that the electropositive cations (Rb^{1+}in $RbTiP_2O_7$ and Ba^{2+} in $BaTi_2(P_2O_7)_2$) not only induce the trivalent oxidation state of the titanium cation but also greatly govern the formation of the $Ti(P_2O_7)_nO_{6-2n}$ unit. Furthermore, the formation of the $Ti(P_2O_7)_nO_{6-2n}$ unit has been observed in a large collection of compounds, $A^IMP_2O_7$ and $A^{II}M_2(P_2O_7)_2$, where M = Ti, V, and Mo [(*2, 3, 8, 9*), and references cited therein]. The α-$NaTiP_2O_7$, however, is the only exception which shows no bidentate pyrophosphate connection with respect to TiO_6 octahedron. Last, the formation of lithium, potassium, rubidium, and cesium pyrophosphates completes the compound series $A^ITiP_2O_7$.

Acknowledgments

This research was supported by the Petroleum Research Fund, administered by the ACS (Grant ACS-PRF 21154-G3), and in part by a Rice University startup grant. Financial support for the single crystal X-ray diffractometer by the National Science Foundation is gratefully acknowledged.

References

1. SHUMIN WANG AND SHIOU-JYH HWU, *J. Solid State Chem.* **90,** 31 (1991).
2. A. LECLAIRE, A. BENMOUSSA, M. M. BOREL, A. GRANDIN, AND B. RAVEAU, *J. Solid State Chem.* **77,** 299 (1988).
3. $LiTiP_2O_7$: a = 4.891 (1) Å, b = 8.213 (1) Å, c = 6.962 (2) Å, β = 108.84 (2) Å, and V = 264.7 (2) Å^3, monoclinic $P2_1$; S. WANG AND S.-J. HWU, Rice University, Houston, Texas, unpublished research (1990).
4. (a) $LiFeP_2O_7$: E. A. GENKINA, B. A. MAKSIMOV, V. A. TIMOFEEVA, A. B. BYKOV, AND O. K. MEL'NIKOV, *Sov. Phys. Dokl.* **30**(10), 817 (1985); (b) $NaFeP_2O_7$: M. GABELICA-ROBERT, M. GOREAUD, PH. LABBE, AND B. RAVEAU, *J. Solid State Chem.* **45,** 389 (1982); (c) $KFeP_2O_7$: D. RIOU, PH. LABBE, AND M. GOREAUD, *Eur. J. Solid State Inorg. Chem.* **25,** 215 (1988).
5. G. M. SHELDRICK (1985) *in* "Crystallographic Computing 3 (G. M. Sheldrick, C. Krüger, and R. Goddard, Eds.), pp. 175–189, Oxford University Press, London/New York (1985).
6. H. N. NG AND C. CALVO, *Can. J. Chem.* **51,** 2613 (1973).
7. F. TAKUSAGAWA, Ames Laboratory, Iowa State University, Ames, Iowa, unpublished research (1981).
8. (a) $KMoP_2O_7$: A. LECLAIRE, M. M. BOREL, A. GRANDIN, AND B. RAVEAU, *J. Solid State Chem.,* **78,** 220 (1989); (b) $RbMoP_2O_7$: unpublished work, reference cited in K.-H. LII, C. C. WANG, AND J. J. CHEN. *J. Solid State Chem.,* **78,** 93 (1989); (c) $CsMoP_2O_7$: K.-H. LII AND R. C. HAUSHALTER, *Acta Crystallogr. Sect. C* **43,** 2036 (1987).
9. $SrV_2(P_2O_7)_2$: S.-J. HWU AND E. D. WILLIS, *J. Solid State Chem.,* in press (1991).